

# 1 Insect wings and body wall evolved from ancient leg segments

2  
3 Heather S. Bruce\* and Nipam H. Patel

4 Department of Molecular and Cell Biology, University of California, Berkeley, CA

5 \*Correspondence: [hbruce@berkeley.edu](mailto:hbruce@berkeley.edu)

6  
7 **Researchers have long debated the origin of insect wings. One theory proposes that the**  
8 **proximal portion of the ancestral crustacean leg became incorporated into the body<sup>1-3</sup>,**  
9 **which moved the leg's epipod (multi-functional lobe, e.g. gill) dorsally, up onto the back to**  
10 **form insect wings<sup>4</sup>. Another theory proposes that the dorsal insect body wall co-opted**  
11 **crustacean epipod genes to form wings<sup>5</sup>. Alternatively, wings may be derived from both leg**  
12 **and body wall (dual origin)<sup>6</sup>. To determine whether wings can be traced to ancestral, pre-**  
13 **insect structures, or arose by co-option, comparisons are necessary between insects and**  
14 **arthropods more representative of the ancestral state, where the hypothesized proximal leg**  
15 **region is not fused to the body wall. To do so, we examined the function of five leg gap**  
16 **genes in the crustacean *Parhyale hawaiiensis* and compared this to previous functional data**  
17 **from insects. Here we show, using CRISPR-Cas9 mutagenesis, that leg segment deletion**  
18 **phenotypes of all five leg gap genes in *Parhyale* align to those of insects only by including**  
19 **the hypothesized fused ancestral proximal leg region. We also argue that possession of eight**  
20 **leg segments is the ancestral state for crustaceans. Thus, *Parhyale* incorporated one leg**  
21 **segment into the body, which now bears the tergal plate, while insects incorporated two leg**  
22 **segments into the body, the most proximal one bearing the wing. We propose a model**  
23 **wherein much of the body wall of insects, including the entire wing, is derived from these**  
24 **two ancestral proximal leg segments, giving the appearance of a “dual origin”<sup>6-10</sup>. This**  
25 **model explains many observations in favor of either the body wall, epipod, or dual origin of**  
26 **insect wings.**

27  
28  
29 Arthropod appendages are key to their spectacular success, but their incredible diversity  
30 has complicated comparisons between distantly related species. The origin of the most debated  
31 appendage, insect wings, pivots on the alignment of leg segments, because wings may be derived  
32 from an epipod (e.g. gill or plate, Fig. 1b)<sup>11</sup> of ancestral leg segments that fused to the body<sup>4,12</sup>,  
33 or alternatively, may represent a co-option of the epipod-patterning pathway by the insect body  
34 wall<sup>5</sup>, or a combination of both (Clark-Hachtel, accompanying manuscript)<sup>6-10</sup>. To answer this,  
35 functional comparisons are necessary between insects and arthropods more representative of the  
36 ancestral state, where the hypothesized proximal leg region is not fused to the body wall.

37 Towards this aim, we examined five leg gap genes, *Distalless* (*Dll*), *Sp6-9*, *dachshund*  
38 (*dac*), *extradenticle* (*exd*), and *homothorax* (*hth*), in an amphipod crustacean, *Parhyale*  
39 *hawaiiensis*. While we have documented their expression at several developmental stages (Fig.  
40 S1), our comparative analysis does not rely solely on these expression patterns, given that  
41 expression is not always a reliable indication of function, and expression is often temporally  
42 dynamic<sup>13</sup>. Instead, we have systematically knocked out these genes in *Parhyale* using CRISPR-  
43 Cas9 mutagenesis and compared this to our understanding of their function in *Drosophila* and  
44 other insects (Figs. 2, S2).

45 Insects have six leg segments, while *Parhyale* has seven (Fig. 1). In insects, *Dll* is  
46 required for the development of leg segments 2 – 6<sup>14-17</sup>. In *Parhyale*, the canonical *Dll* gene,

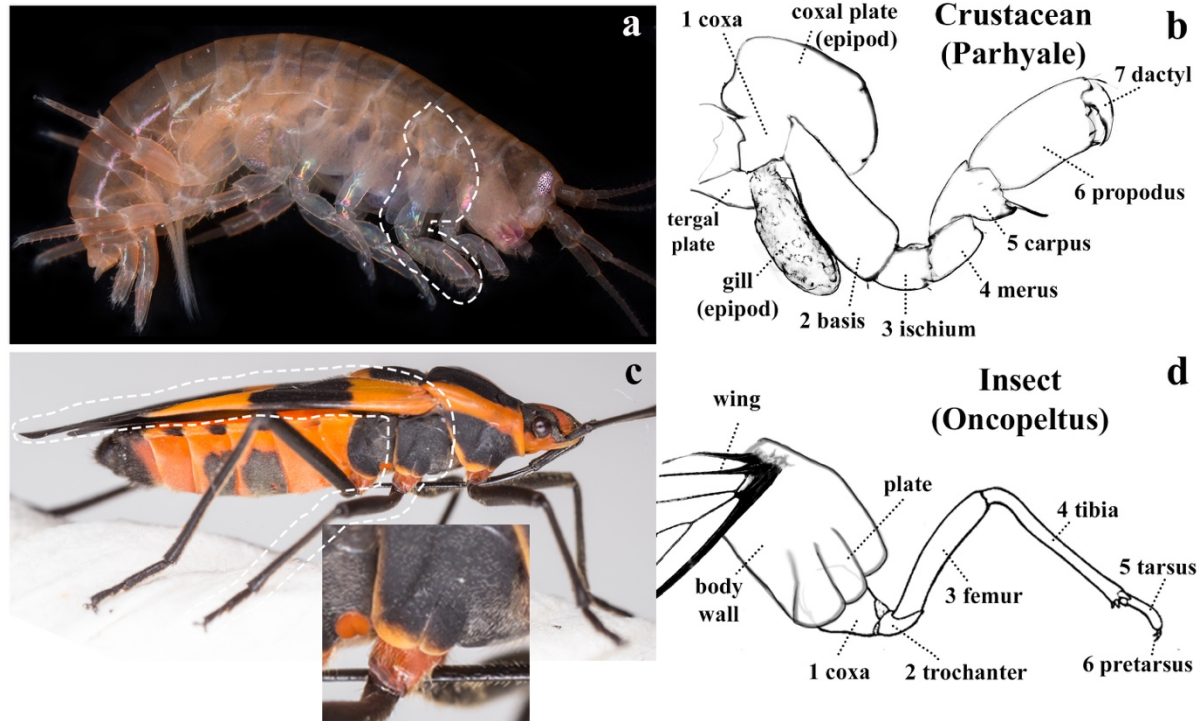


Fig. 1. Crustacean and insect legs. (a) Adult *Parhyale*, with third thoracic leg (T3) outlined. (b) Cartoon of *Parhyale* T3. The coxal plate extends over the leg. (c) Adult *Oncopeltus*, with T2 outlined. Inset shows magnified proximal leg, with body wall plate extending over the leg. (d) Cartoon of *Oncopeltus* T2 leg.

47  
 48 *Dll-e*<sup>18-20</sup>, is required for the development of leg segments 3 – 7 (Fig. 2b). In insects, *Sp6-9*  
 49 is required for the development of leg segments 1 – 6<sup>14,21-23</sup>, and in addition in *Drosophila*, loss of  
 50 *Sp6-9* (i.e. D-*Sp1*<sup>22</sup>) occasionally transforms the leg towards wing and lateral body wall  
 51 identity<sup>23</sup>. In *Parhyale*, *Sp6-9*<sup>22</sup> is required for the development of leg segments 2 – 7 (Fig. 2c),  
 52 and in some legs, segment 2 is occasionally homeotically transformed towards a leg segment 1  
 53 identity (Fig S3). In *Drosophila*, *dac* is required in the trochanter through proximal tarsus (leg  
 54 segments 2 – 4, and first tarsus)<sup>24,25</sup>. *Parhyale* has 2 *dac* paralogs. *Dac1* does not seem to be  
 55 expressed in the legs or have a knockout phenotype. *Dac2* is required to pattern leg segments 3 –  
 56 5 (Fig. 2d). *Exd* and *hth* are expressed in the body wall and proximal leg segments of insects<sup>26-29</sup>  
 57 and *Parhyale*<sup>30</sup> (Fig S1). They form heterodimers<sup>31</sup> and therefore have similar phenotypes<sup>26-29</sup>. In  
 58 insects, *exd* or *hth* knockout results in deletions/fusions of the coxa through proximal tibia (leg  
 59 segments 1 – 3, and proximal tibia)<sup>26-29</sup>. In *Parhyale*, *exd* or *hth* knockout results in  
 60 deletions/fusions of the coxa through proximal carpus (leg segments 1 – 4, and proximal carpus;  
 61 Figs. 2e, f). In both insects<sup>26,27,32</sup> and *Parhyale*, the remaining distal leg segments are sometimes  
 62 transformed towards a generalized thoracic leg identity (compare Fig. 2 e, f and Fig S4). In both  
 63 insects<sup>26-29</sup> and *Parhyale* (Fig. S4), *exd* or *hth* knockout results in deletions/fusions of body  
 64 segments.

65 In summary, the expression and function of *Dll*, *Sp6-9*, *dac*, *exd*, and *hth* in *Parhyale* are  
 66 shifted distally by one segment relative to insects. This shift is accounted for if insects fused an  
 67 ancestral proximal leg segment to the body wall (Fig. 2g). Thus, there is a one-to-one homology  
 68 between insect and *Parhyale* legs, displaced by one segment, such that the insect coxa is  
 69 homologous to the crustacean basis, the insect femur is the crustacean ischium, and so on for all

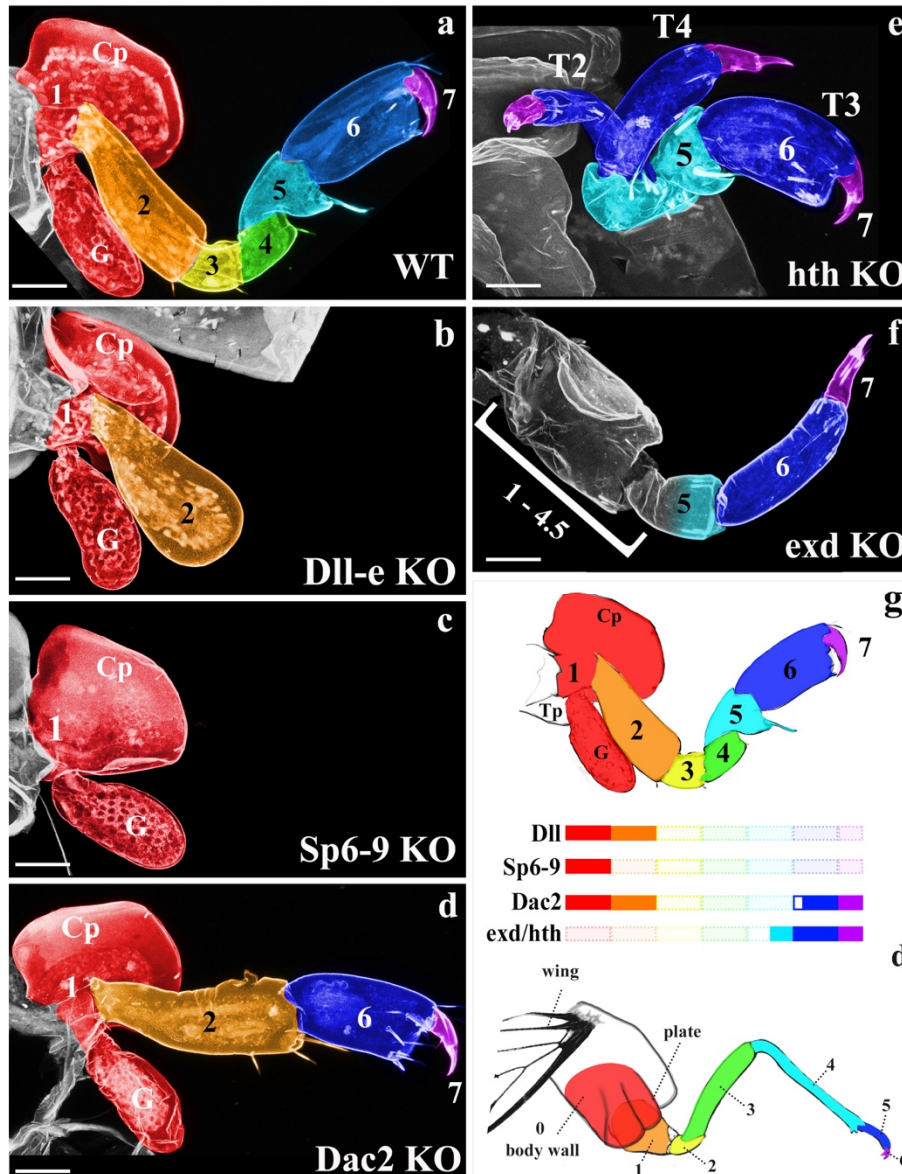
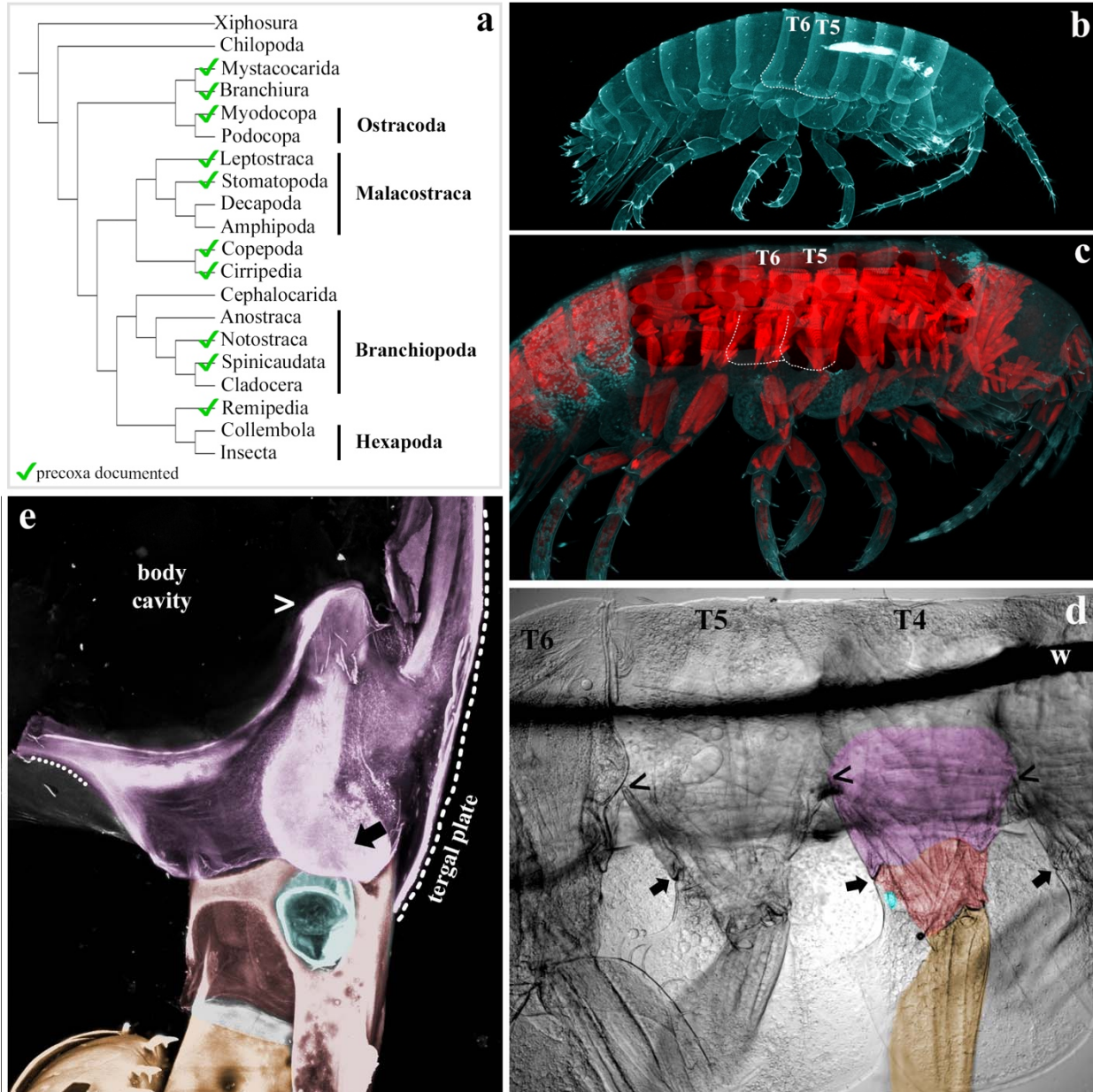


Fig. 2. Knockout phenotypes of leg gap genes. (a-f) *Parhyale* CRISPR-Cas9 phenotypes in dissected third thoracic legs (T3). Graded cyan in f indicates deletion/fusion of proximal leg segment 5. (g) Leg gap gene function in *Parhyale* and insects aligns only if insects incorporated the red leg segment into the body wall (0). Color bars correspond to remaining leg segments following knockout, transparent bars indicate deleted leg segments. Open bar in *dac* indicates slight extension of *dac* function into tarsus 1 of insects. Coxal plate (Cp), gill (G), tergal plate (Tp). Scale bar 50um.

70

71 leg segments. This also means that at least part of the insect body wall is homologous to the  
72 crustacean coxa.

73 The data thus far is agnostic regarding the origin of the insect wing. However, we noted  
74 that *Parhyale* has what appears to be an epipod, the tergal plate, emerging proximal to the coxa.  
75 Clark-Hachtel (accompanying manuscript) show that the tergal plate, coxal plate, and basal plate  
76 all require the same “wing” genes, indicating that all three are epipods. They also show that  
77 nubbin, a marker of arthropod leg joints, is expressed in a distinct stripe above the *Parhyale*  
78 tergal plate, suggesting there is a leg segment here. An examination of the crustacean appendage  
79 morphology literature in the context of recent phylogenies shows that most crustaceans in fact  
80 have an additional proximal leg segment, the precoxa (Fig. 3a), and that the presence of a  
81 precoxa is the ancestral state. Although a precoxa has not been previously documented in  
82 amphipods, a careful examination using confocal and bright field microscopy reveals that  
83 *Parhyale* has a structure between the coxa and body wall that meets the criteria for a leg



84 segment: it protrudes from the body wall; it forms a true, muscled joint; and it extends  
 85 musculature to another leg segment (Figs. 3 and S5)<sup>12,33,34</sup>. Furthermore, the tergal plate emerges  
 86 not from the body wall, but from this precoxa (Fig. 3e). Thus, much of what appears to be lateral  
 87 body wall in *Parhyale* is in fact proximal leg.

88 Since insects evolved from crustaceans, if the insect coxa is homologous to the  
 89 crustacean basis, then one would expect to find two leg segments incorporated into the insect  
 90 body wall, each equipped with an epipod (Fig. 4). As predicted, two leg-like segments can be  
 91 observed proximal to the coxa in basal hexapods<sup>2</sup> including collembolans<sup>35</sup>, as well as in the  
 92 embryos of many insects<sup>9,36,37</sup>. In insect embryos, these two leg-like segments flatten out before  
 93 hatching to form the lateral body wall<sup>2,3,9,35-38</sup> (Fig 1c). Furthermore, insects indeed have two  
 94 epipods proximal to the insect coxa. When “wing” genes are depleted in insects via RNAi, two  
 95 distinct regions are affected: the wing, but also the protruding plate adjacent to the leg

96 < Fig. 3. *Parhyale* has a precoxa. (a) Phylogeny based on Oakley 2012, precoxa references in  
97 supplements. (b) Confocal of *Parhyale* hatchling. Round T5 tergal plate and pointy T6 tergal  
98 plate (dashed outlines). (c) Confocal of *Parhyale* hatchling, cuticle in cyan, muscle in red. Note  
99 the blocks of simple, anterior-posterior muscles of the body vs the orthogonal, complexly  
100 arranged muscles of the leg segments. Outline of tergal plates (dashed line) relative to orthogonal  
101 muscle. (d) BF image of right half of adult *Parhyale*, sagittal dissection, innards removed, lateral  
102 view. Wire used to position sample (w). The same orthogonal muscles in b are visible as  
103 striations that continue above the wire. The precoxa forms a joint with the coxa, including a  
104 gliding articulation (arrow). The dorsal limit of the precoxa is unclear, but the most conservative  
105 estimate is to begin at the gliding joint (arrow) and follow the leg up to where it meets the  
106 adjacent leg, denoted by (<). By comparing (<) and (→), it can be seen that the precoxa  
107 protrudes quite a bit from the body wall. However, the precoxa appears to continue farther up the  
108 body wall (compare orthogonal muscle striations). (e) Posterior-lateral view of right T6, looking  
109 edge-on at tergal plate. The tergal plate (dotted outline) emerges from the precoxa (contiguous  
110 pink between ←, →, and ---). In c, d, coxa is red (coxal plate not shaded, to focus on joints), gills  
111 (teal) partially cut for visibility, basis is orange, precoxa is pink. Note that all three plates (tergal,  
112 coxal, and basal) form contiguous cuticle with their leg segment, i.e. there is no distinguishing  
113 suture.

114  
115

116 (Fig. 1c)<sup>39-42</sup>. These data are explained if insects incorporated the ancestral precoxa and  
117 crustacean coxa into the body wall, with the precoxa epipod later forming the wing and the  
118 crustacean coxa epipod later forming the plate.

119 The results presented here may settle a long-standing debate concerning the origin of  
120 insect wings as derived from (a) the epipod of the leg, (b) the body wall, or, more recently, (c)  
121 from both (dual-origin hypothesis; see Clark-Hachtel, accompanying manuscript)<sup>6</sup>. Our model  
122 accounts for all observations in favor of either the body wall or epipod origin of insect wing  
123 evolution, including the dorsal position of insect wings relative to their legs, the loss of ancestral  
124 leg segments in insects, the two-segmented morphology of the insect subcoxa in both embryos  
125 and adults, the complex musculature for flight, and the shared gene expression between wings  
126 and epipods. The realization that crustaceans have a precoxa accounts for the apparent “dual  
127 origin” of insect wings: much of what appears to be insect body wall is in fact the crustacean  
128 precoxa.

129 In fact, a number leg-associated outgrowths in arthropods are explained by this model, in  
130 addition to insect wings. The *Daphnia* carapace<sup>43</sup> is the epipod of the precoxa{Hansen:1925tba};  
131 the *Oncopeltus* small plate outgrowth (Fig. 1c) is the epipod of the crustacean coxa; and the  
132 thoracic stylus of jumping bristletails (Fig. 4, st) is the epipod of the crustacean basis<sup>10,44</sup>. This  
133 also explains many insect abdominal appendages, like gills<sup>45</sup>, gin traps<sup>40</sup>, prolegs<sup>46</sup>, and sepsid  
134 fly appendages<sup>47</sup>, which are often proposed as de novo structures<sup>48-50</sup>. However, most insects  
135 form abdominal appendages as embryos<sup>45,51</sup>, some even with an epipod nub, but these fuse to the  
136 body wall before hatching to form the sternites<sup>37</sup>. This is supported by a re-analysis of the  
137 expression of *Sp6-9* and its paralog, *buttonhead*, in insect embryos<sup>22</sup>. According to the leg  
138 segment homology model presented here (Fig. 4), the paired dots of *btd* expression in each  
139 abdominal segment of insect embryos demonstrates that these appendages are comprised of a  
140 minimum of three leg segments: the precoxa (pink), crustacean coxa (red), and insect coxa  
141 (orange). Thus, rather than de novo co-options, abdominal appendages were always there,

142 persisting in a truncated, highly modified state, and de-repressed in various lineages to form  
 143 apparently novel structures. This provides a model for how insect wings can be both homologous  
 144 to the epipod of the crustacean precoxa, and yet not be continuously present in the fossil record:  
 145 epipod fields may persist in a truncated state, perhaps only visible as a nub in the embryo. We  
 146 propose this as a general mechanism for the origin of novel structures that appear to be derived  
 147 from serial homologs, rather than co-option.

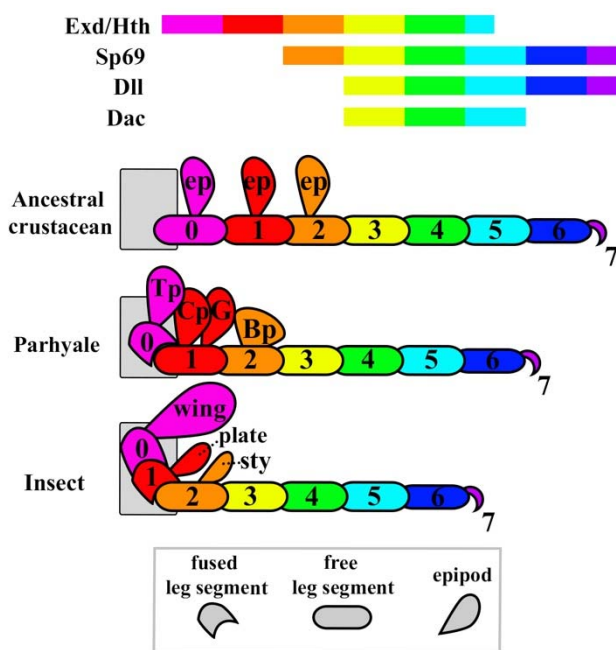
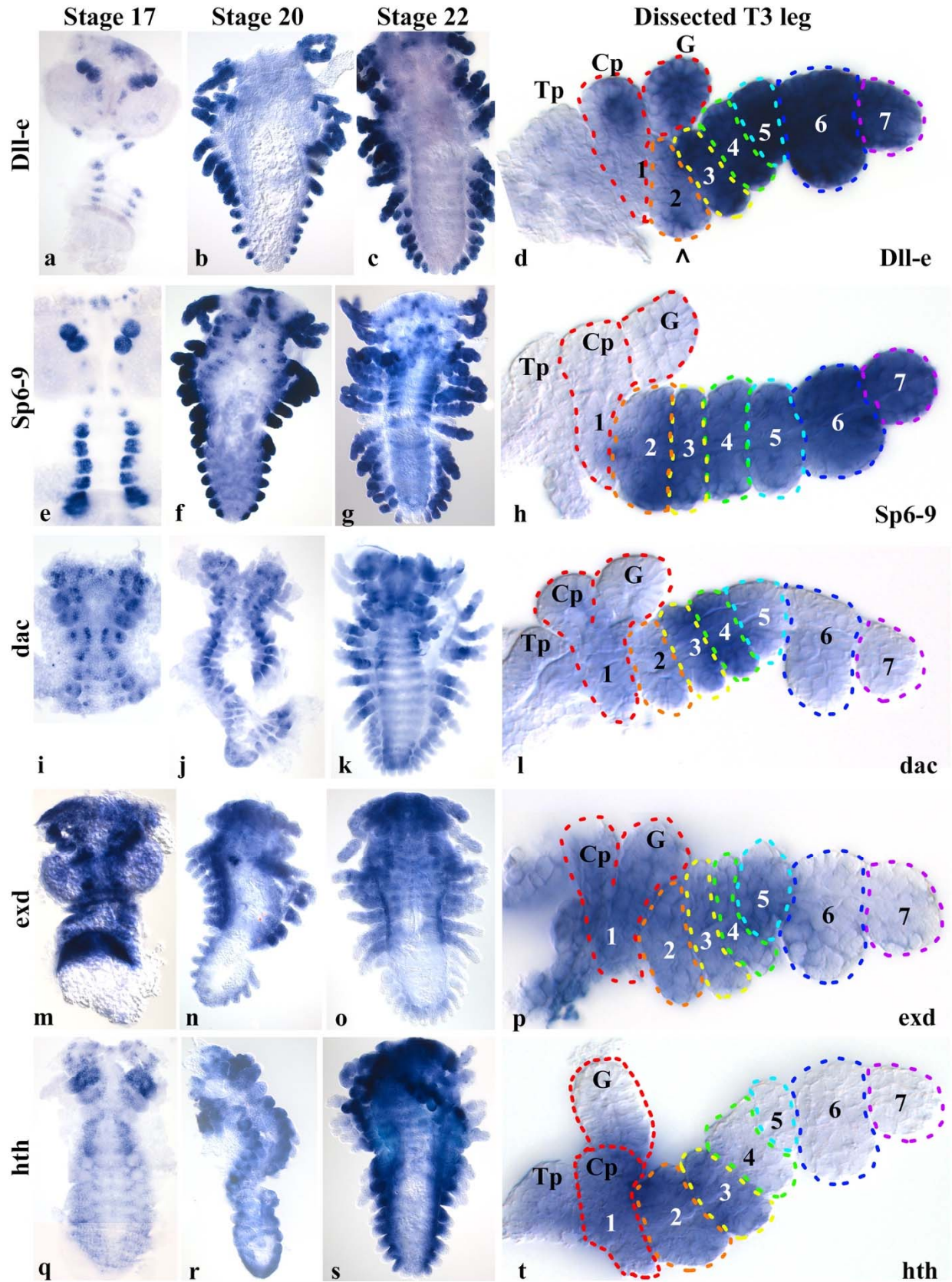


Fig 4. Gene expression alignment and proposed leg segment homologies (colors) between an ancestral crustacean, *Parhyale*, and insects. Ancestral precoxa epipod (ep), *Parhyale* tergal plate (Tp), and insect wing are homologous (pink). Ancestral coxa epipod, *Parhyale* coxal plate (Cp) and gill (G), and insect plate (see Fig. 1c) are homologous (red). Ancestral basis epipod, *Parhyale* basal plate (Bp), and jumping bristletail stylus (sty) are homologous (orange).



^ Fig S1. Expression of leg gap genes in whole embryos and dissected third thoracic legs (T3). (a – d): *Dll-e*. (e – h): *Sp6-9*. (i – l): *dac2*. (m – p): *exd*. (q – t): *hth*. Embryonic expression data for *Dll-e*<sup>18-20</sup>, *Sp6-9*<sup>22</sup>, and *exd* and *hth*<sup>30</sup> have been previously characterized, but not at the level of individual leg segments. (d) *Dll-e* is expressed in leg segments 3 – 7; in the interior of the tergal plate (Tp), coxal plate (Cp), and gill (G), where it may be playing a sensory role, similar to the expression of Dll that patterns sensory hairs in the *Drosophila* wing margin<sup>15</sup>; and marks the bristle (^) of leg segment 2. This bristle is deleted in *Dll-e* KO (compare Fig. 2a, b). (h) *Sp6-9* is expressed in leg segments 2 – 7. (l) *dac2* is expressed in leg segments 3 – 5. Expression in segment 5 may be stronger at other time points. (p) *exd* is expressed in the body wall through leg segment 5, and perhaps a little in 6. *Exd* is not expressed in the gill (not visible here). (t) *hth* is expressed in the body wall through leg segment 3. *Hth* is not expressed in the gill. Note that both insects and *Parhyale* share a peculiar disparity between *hth* expression and function, wherein *hth* knockout deletes one more leg segment than would be predicted by the *hth* expression domain.

149  
150  
151  
152  
153  
154  
155  
156  
157  
158  
159  
160



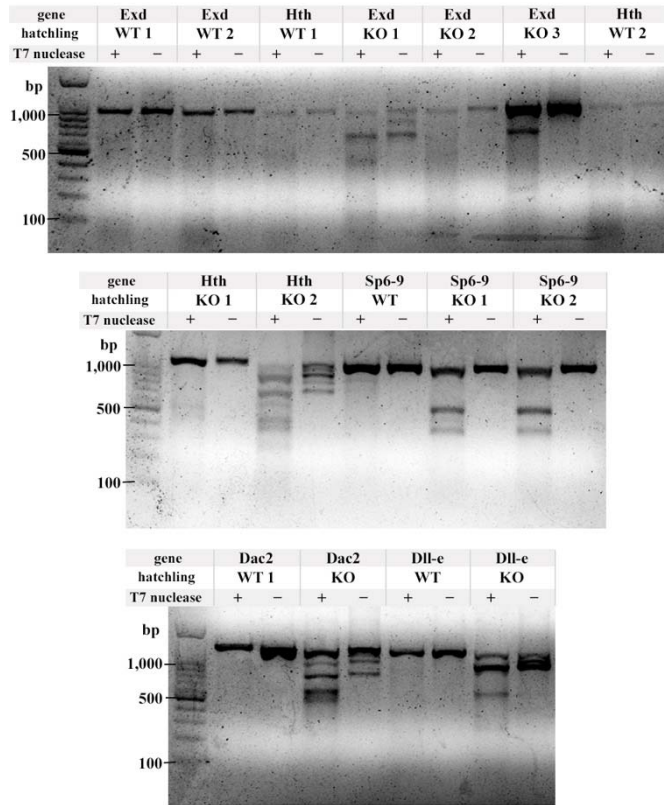


Fig. S2. T7 endonuclease assay to confirm CRISPR-Cas9 mutagenesis. For each gene, one or two wild type (WT) hatchlings were assayed, and one, two, or three KO hatchlings were assayed. T7 endonuclease was either added (+) or not added (-) to the heteroduplex mixture. In brief, a ~1kb region flanking the CRISPR-Cas9 target site by at least 300bp to either side was amplified by PCR from either WT or KO hatchlings. The purified PCR products were denatured, then slowly cooled to allow WT DNA and mutant DNA with indels to anneal, resulting in a “bubble” of unpaired DNA (heteroduplex) at the target site. T7 endonuclease was added to the (+) samples, incubated, and run on a 1.5% agarose gel. KO animals are mosaic, so if the target site was cut, the indels will cause heteroduplexes when annealed with either a WT strand, or a different indel. When a single deletion is present, each half of the cut heteroduplex adds up to approximately 1kb (see *Sp6-9* KO 1 and 2). Some deletions are large enough to be seen without the T7 endonuclease assay (see *Dll-e* KO), and some hatchlings had multiple deletions which produced multiple bands when cut with T7 (see *exd* KO 1, *hth* KO 2, *dac2* KO).

161

162

Gene	sgRNA	total injected	# dead	death %	# hatch w/phenotype	% phenotype of hatched
<i>Dll-e</i>	1+2	151	45	30%	57	54%
<i>exd</i>	1+2	206	90	44%	86	74%
<i>exd</i>	1	204	102	50%	84	82%
<i>exd</i>	2	173	36	21%	85	62%
<i>hth</i>	1+2	124	71	57%	32	60%
<i>hth</i>	1	131	30	23%	36	36%
<i>hth</i>	2	99	62	63%	22	59%
<i>dac2</i>	1+2	80	28	35%	41	79%
<i>dac2</i>	1	84	31	37%	9	17%
<i>dac2</i>	2	88	18	20%	16	23%
<i>Sp6-9</i>	1+2	165	88	53%	51	66%
<i>Sp6-9</i>	1	54	22	41%	9	28%
<i>Sp6-9</i>	2	37	3	8%	15	44%

Table 1. CRISPR-Cas9 injection numbers. Two sgRNAs per gene were made, and either one or both were injected as indicated. Both guides for each gene gave the same phenotype. # dead is the number of embryos that did not survive to hatching. For each gene, sgRNA 1 and 2 produced the same phenotypes.

163  
164  
165  
166  
167  
168  
169  
170  
171

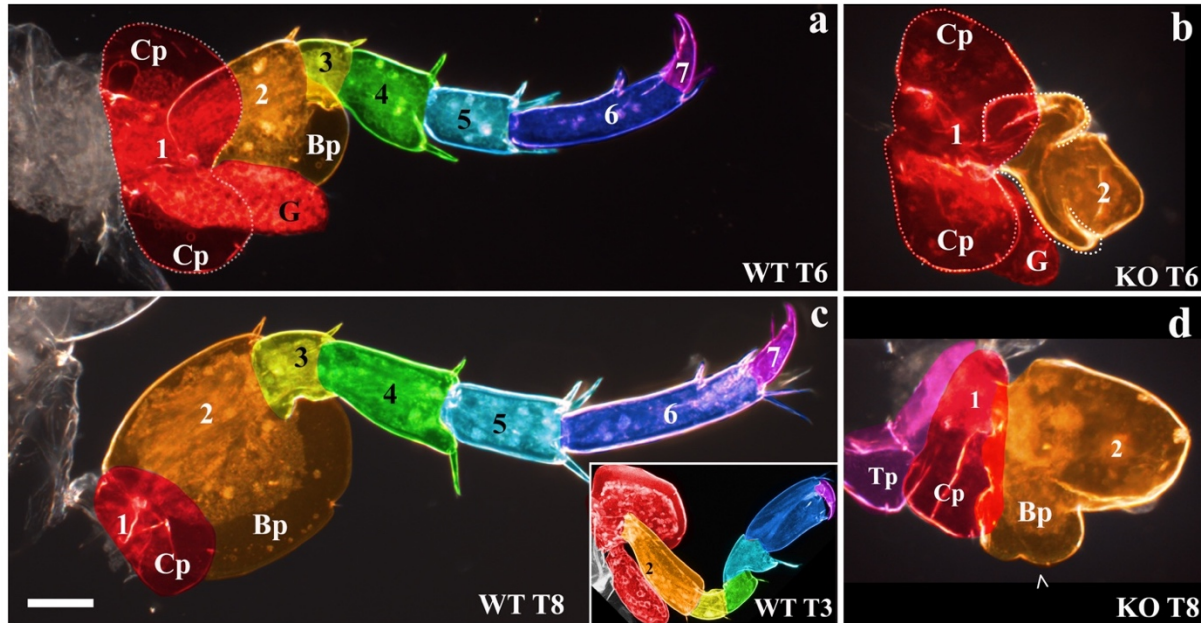


Fig S3. *Sp6-9* knockout sometimes causes a homeotic transformation of orange leg segment 2 towards a red leg segment 1 identity in jumping legs (thoracic legs T6 – 8). In WT jumping legs (a, c), orange leg segment 2 is very large and wide, due to the epipod on this segment (compare to skinny orange leg segment of WT T3 leg, inset in c). In WT T6 legs (a), the red coxal plate is bilobed, while in the WT T8 legs (c), the coxal plate is small and oval. In T6 *Sp6-9* KO (b), the epipod of orange leg segment 2 is bilobed, indicating a transformation towards red leg segment 1. In T8 *Sp6-9* KO (d), the large epipod of orange leg segment 2 has been reduced to the size and shape of the coxal plate, indicating a transformation towards red leg segment 1. Note that the tergal plates are unaffected (d, pink, Tp), which is similar to *Drosophila Sp6-9* knockouts, where the wings are unaffected<sup>23</sup>. The bilobed shape of the transformed T6 basal plate demonstrates that these are transformations towards a coxal plate rather than tergal plate, because the tergal plates are never bilobed. Therefore, these represent a homeotic transformation of one leg segment into another. This argues that the transformation of *Drosophila* leg to wing following loss of *Sp6-9* is also a transformation of one leg segment into another, and thus that insect wings are appendicular. Scale bar 50um.

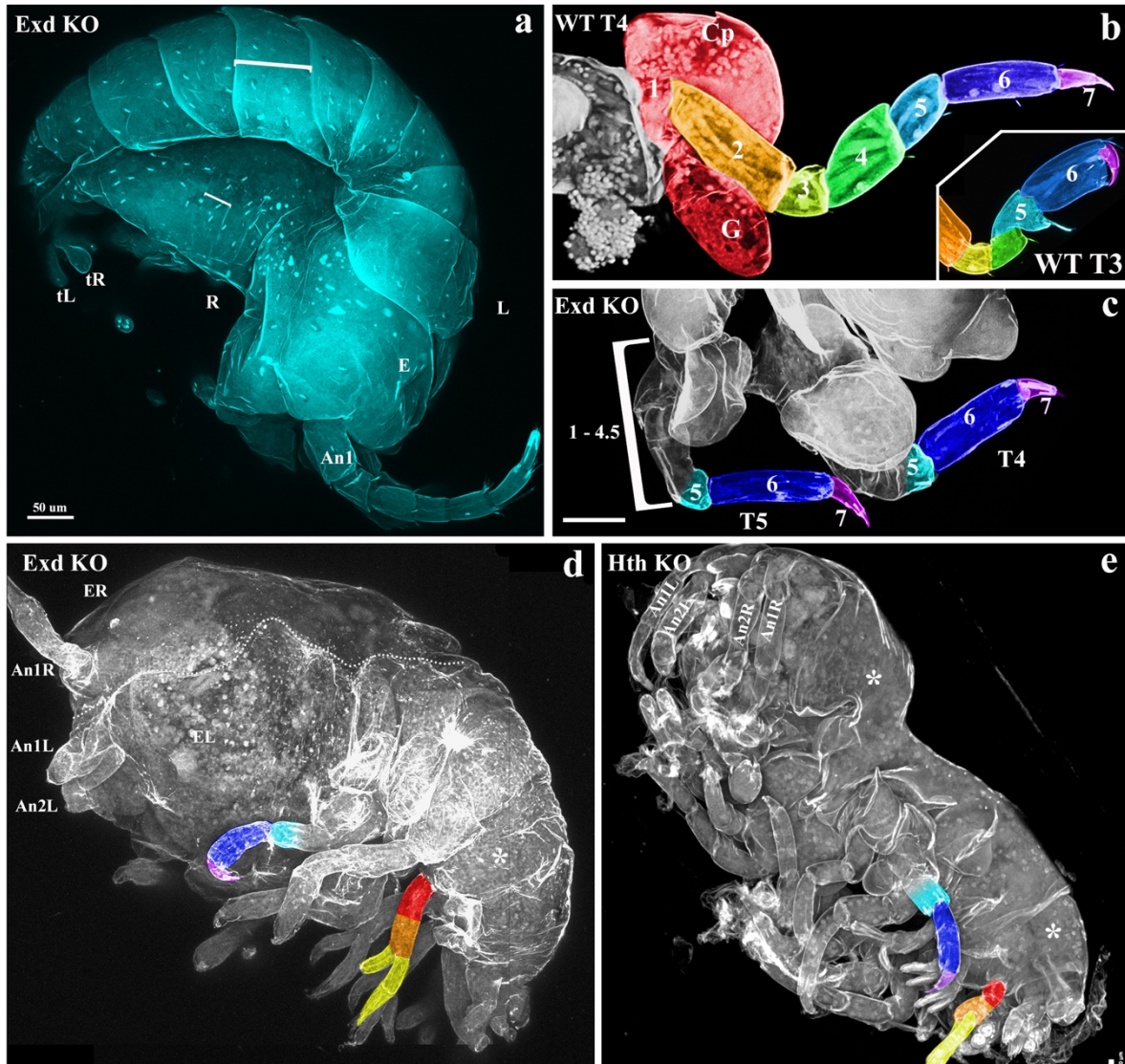


Fig. S4. *Exd* and *hth* phenotypes continued. (a) Body segment fusions/deletions in *exd* knockout whole hatchling. Confocal of unilaterally affected hatchling, dorsal view, anterior at bottom, posterior at left. Left side of animal (L) appears WT. The foreshortening of only the right (R) half of the body results in hatchlings with bodies twisted laterally into a nearly spiral shape. The tissue where the eye (E) would have been located is deleted, leaving a recess. Left first antenna (An1), left and right telson (tL, tR). White brackets compare the length of the body segments in right fused and left unfused segments. (b) WT T4 leg. Inset, WT T3 leg. Note broad shape of WT T3 blue leg segment 6 to skinny shape in WT T4/5. Also note triangle shape of WT T3 cyan leg segment 5 vs cylinder shape in WT T4/5, and presence of bristle in T3. (c) *exd* KO T4 and T5 legs. Loss of *exd* deletes/fuses leg segments 1 – 4 and proximal 5, leaving the distal half of leg segment 5 (indicated by fading cyan), and all of leg segments 6 and 7. Note that the joint between leg segments 5 and 6 is normal, but there is no apparent joint on the proximal side of leg segment 5. *Exd* KO also transforms the remaining T3 leg segments towards a T4/5 identity: *exd* KO T3 blue leg segment 6 is skinny, and cyan leg segment 5 is cylindrical and lacks the bristle (see Fig 2f). (d) Lateral view of *exd* KO hatchling. Hatchling died before cuticle growth. Dorsal midline indicated

with dashed white line. Left and right positions of eye in WT animals (EL, ER). (e) Lateral view of *hth* KO hatchling. *Exd* and *hth* KO produce the same body segment deletions/fusions, indicated with (\*), compare to WT body segments in a, Left side, and in Figs. 1A and 3B. Neither *exd* nor *hth* KO appears to affect abdominal legs, because all abdominal proximal leg segments (red and orange) are intact in the same severely affected hatchlings where all thoracic proximal leg segments are deleted/fused, leaving only the distal thoracic leg segments (cyan, blue, purple). Lack of phenotype in abdominal legs is not due to knockout mosaicism: *exd* and *hth* are indeed knocked out in the abdomens of these hatchlings, because the body segments of the abdomen are fused together (\*). Antenna (An).

172  
173  
174  
175  
176  
177  
178  
179  
180  
181  
182  
183  
184  
185  
186  
187  
188  
189  
190  
191  
192  
193  
194  
195  
196  
197  
198  
199  
200  
201  
202  
203  
204  
205  
206  
207

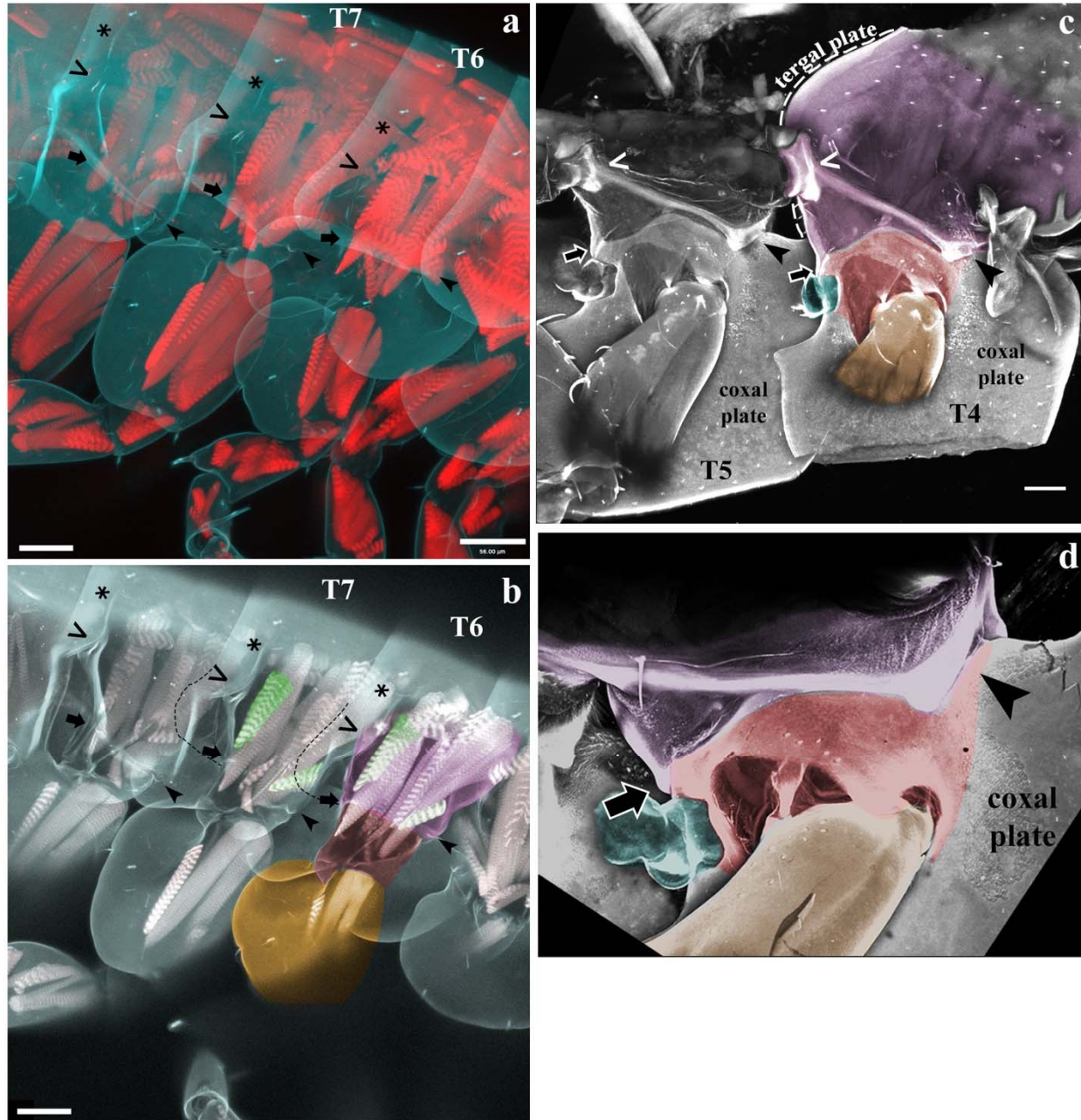


Fig. S5. *Parhyale* precoxa forms a true, muscled joint and extends musculature to another leg segment. Confocal images. (a) Phalloidin stain of muscle in right half of *Parhyale* hatchling. Contrast simple, anterior-posterior body muscles to orthogonal, complexly arranged leg muscles. No muscles cross the coxa-basis joint, as noted by Boxshall 1998. Note that all three plates (tergal, coxal, and basal) form contiguous cuticle with their leg segment, i.e. there is no distinguishing suture. (b) Optical section showing superficial muscles of right half. Confocal colors are partially desaturated: cuticle in grey-blue, muscle in grey-pink. The precoxa forms two articulations with the coxa: an anterior, bifurcated, load-bearing hinge articulation (arrowhead), and a posterior gliding articulation ( $\rightarrow$ ) (see also Fig. 3e). Coxa is red (coxal plate not shaded, to focus on joints), basis is orange, precoxa is magenta pink. Adjacent legs meet on their ventral sides at ( $<$ ) and on their dorsal sides at (\*). Outline of tergal plate (dashed line) relative to muscle

and joints shows that tergal plate emerges from precoxa. Muscles in green insert on the precoxa-coxa joint, indicating that this is a true joint, and not merely a point of flexure in the exoskeleton (annulation)<sup>12,33,34</sup>. The shorter, anterior muscle originates in the protruding precoxa to insert on the rim of the next leg segment, the coxa. This muscle is therefore an intrinsic muscle, a hallmark of a true leg segment<sup>12,33,34</sup>. (c) Confocal of dissected left half, medial view. Coxal plate and basis partially cut. The precoxa forms a joint with two articulations with the coxa: an anterior, bifurcated, load-bearing hinge articulation (arrowhead), and a posterior gliding articulation (arrow). Orthogonal muscles visible as striations on T4 precoxa. (d) Close-up of left T4, medial-anterior view, showing bifurcated hinge articulation.

208  
209  
210  
211  
212  
213  
214  
215  
216  
217  
218  
219  
220  
221  
222  
223  
224  
225  
226  
227  
228  
229  
230  
231  
232  
233  
234  
235  
236  
237  
238  
239  
240  
241  
242  
243  
244

245  
246  
247  
248  
249  
250  
251  
252  
253  
254  
255  
256  
257  
258  
259  
260  
261  
262  
263  
264  
265  
266  
267  
268  
269  
270  
271  
272  
273

## METHODS

### BIOINFORMATICS

Partial or complete sequences for *Parhyale Dll*, *Sp6-9*, *Exd*, and *Hth* have been previously identified. These were >99% identical at the nucleotide level to sequences in the *Parhyale* assembled transcriptome. In order to confirm their orthology, identify potential *Parhyale* paralogs and identify *Parhyale dac*, we ran reciprocal best Blast hit searches. For each gene, orthologs from several arthropods and vertebrates were downloaded from NCBI and EMBL and aligned against the *Parhyale* transcriptome<sup>52</sup> using standalone NCBI blastp. The *Parhyale* hits with the lowest E-values were used to run a blastp against the NCBI database, restricted to Arthropoda. We confirmed that the original set of orthologs from several arthropods were the best hits to our *Parhyale* candidates (i.e. were each other's reciprocal best Blast hits). These reciprocal best Blast hits are listed in the tables below, and were deposited in Genbank under Accession Numbers MG457799 - MG457804.

No *Parhyale* buttonhead/Sp5 was recovered in the assembled transcriptome. Buttonhead/Sp5 was also not found in the genome of the related amphipod *Hyaella azteca*. The assembled transcriptome only recovered fragments of *Parhyale* Sp1-4, so the previously sequenced *Parhyale* Sp1-4 (CBH30980.1) was used for the table below (asterisk).

*Parhyale* has three *Dll* paralogs, which appear to be an amphipod-specific duplication, because a related amphipod, *Hyaella azteca*, also has these same three *Dll* paralogs. The three *Parhyale* *Dll* paralogs had the lowest E-values to all *Dll* orthologs examined, but which of the three *Parhyale* *Dll* paralogs had the lowest E-value was variable, as expected for a clade-specific duplication.

The coding region for *Parhyale* *exd* and *hth* in the assembled transcriptome are longer than those previously identified. *Exd* is 204 amino acids longer, and *hth* is 166 amino acids longer. This explains the higher-than-expected E-values between the *Parhyale* *exd* and *hth* sequences identified previously and the *Parhyale* *exd* and *hth* sequences used in this study.

Extradenticle		
Query id	Subject id	E-value
Daphnia_pulex exd EFX62563.1	<i>Parhyale</i> exd MG457802	8.00E-177
Drosophila exd AAF48555.1	<i>Parhyale</i> exd MG457802	7.00E-173
Hyaella exd XP_018011298.1	<i>Parhyale</i> exd MG457802	2.00E-166
<i>Parhyale</i> exd CAO98909.1	<i>Parhyale</i> exd MG457802	6.00E-126
Tribolium exd NP_001034501.1	<i>Parhyale</i> exd MG457802	1.00E-173
Homo Pbx1 NP_002576.1	<i>Parhyale</i> exd MG457802	3.00E-166

274  
275

Homothorax		
Query id	Subject id	E-value
Daphnia hth EFX75948.1	<i>Parhyale</i> hth MG457803	0
Drosophila hth NP_476578.3	<i>Parhyale</i> hth MG457803	6.00E-179
Homo Meis2 AAH07202.1	<i>Parhyale</i> hth MG457803	1.00E-148



Hyaella hth XP_018016731.1	<i>Parhyale</i> hth MG457803	0
<i>Parhyale</i> hth CAO98908.1	<i>Parhyale</i> hth MG457803	0
Tribolium hth NP_001034489.1	<i>Parhyale</i> hth MG457803	0

276  
277

Sp6-9, Sp1-4, buttonhead/Sp5		
Query id	Subject id	E-value
Drosophila btd NP_511100.1	<i>Parhyale</i> Sp6-9 MG457804	4.00E-47
Drosophila Sp1-4 NM_142975.3	* <i>Parhyale</i> Sp1-4 CBH30980.1	5.00E-62
Drosophila Sp6-9 NP_727360.1	<i>Parhyale</i> Sp6-9 MG457804	6.00E-109
Homo Sp4 NP_003103.2	* <i>Parhyale</i> Sp1-4 CBH30980.1	2.00E-66
Homo Sp5 NP_001003845.1	<i>Parhyale</i> Sp6-9 MG457804	7.00E-62
Homo Sp8 NP_874359.2	<i>Parhyale</i> Sp6-9 MG457804	3.00E-105
Hyaella Sp1-4 XP_018012207.1	* <i>Parhyale</i> Sp1-4 CBH30980.1	0
Hyaella Sp6-9 XP_018014881.1	<i>Parhyale</i> Sp6-9 MG457804	0
<i>Parhyale</i> Sp1-4 CBH30980.1	* <i>Parhyale</i> Sp1-4 CBH30980.1	0
<i>Parhyale</i> Sp6-9 CBH30981.1	<i>Parhyale</i> Sp6-9 MG457804	0
Tribolium btd NP_001107792.1	<i>Parhyale</i> Sp6-9 MG457804	7.00E-59
Tribolium Sp1-4 XP_015833716.1	<i>Parhyale</i> Sp6-9 MG457804	3.00E-62
Tribolium Sp6-9 XP_008198341.1	<i>Parhyale</i> Sp6-9 MG457804	6.00E-159

278  
279

Distalless		
Query id	Subject id	E-value
Drosophila Dll ACL83212.1	PhDII2	2.00E-54
Drosophila Dll ACL83212.1	PhDII1	2.00E-48
Drosophila Dll ACL83212.1	PhDIIe MG457801	4.00E-42
Homo DLX-2 AAB40902.1	PhDIIe MG457801	3.00E-35
Homo DLX-2 AAB40902.1	PhDII2	6.00E-35
Homo DLX-2 AAB40902.1	PhDII1	3.00E-34
Hyaella DLX-2 XP_018023955.1	PhDIIe MG457801	0
Hyaella DLX-2 XP_018023955.1	PhDII1	1.00E-49
Hyaella DLX-2 XP_018023955.1	PhDII2	3.00E-45
Hyaella DLX-6 XP_018023956.1	PhDII2	4.00E-102
Hyaella DLX-6 XP_018023956.1	PhDII1	1.00E-51
Hyaella DLX-6 XP_018023956.1	PhDIIe MG457801	1.00E-40
Hyaella unchar. protein XP_018023484.1	PhDII1	8.00E-83
Hyaella unchar. protein XP_018023484.1	PhDII2	0.89
<i>Parhyale</i> Dll-e ACT78885.1	PhDIIe MG457801	0

<i>Parhyale</i> DII-e ACT78885.1	PhDII1	7.00E-48
<i>Parhyale</i> DII-e ACT78885.1	PhDII2	1.00E-44
<i>Tribolium</i> DII AAG39634.1	PhDII1	7.00E-48
<i>Tribolium</i> DII AAG39634.1	PhDII2	1.00E-46
<i>Tribolium</i> DII AAG39634.1	PhDIIe MG457801	5.00E-39

280  
281

Dachshund		
Query id	Subject id	E-value
<i>Daphnia pulex</i> dac EFX90187.1	<i>Parhyale</i> Dac1 MG457799	3.00E-67
<i>Drosophila</i> dac AAF53538.3	<i>Parhyale</i> Dac2 MG457800	2.00E-64
Homo dach2 Q96NX9	<i>Parhyale</i> Dac1 MG457799	4.00E-52
<i>Hyaella</i> Dac1 XP_018011787.1	<i>Parhyale</i> Dac1 MG457799	7.00E-109
<i>Hyaella</i> Dac1 XP_018011787.1	<i>Parhyale</i> Dac2 MG457800	2.00E-55
<i>Hyaella</i> Dac2 XP_018011801.1	<i>Parhyale</i> Dac2 MG457800	0
<i>Hyaella</i> Dac2 XP_018011801.1	<i>Parhyale</i> Dac1 MG457799	1.00E-59
<i>Tribolium</i> dac1 XP_015834662.1	<i>Parhyale</i> Dac2 MG457800	6.00E-72

282  
283  
284  
285  
286

#### IN SITU PRIMER SEQUENCES

Primer name	product size	seq
hth FORWARD	941	GTTATGGGCTCCGTACCTGA
hth REVERSE	941	GCCAGCTGTTTCTTCTGGTC
exd FORWARD	734	AGCGAGTCCTCAACAAAGGA
exd REVERSE	734	AGGAGGCGTGTGCTATTCTG
DII FORWARD	725	TGGGTCCAGTTCAACCTCTC
DII REVERSE	725	GACATCGTCCTCCAAAGCAT
dac 1 FORWARD	638	GGAGAGCAGAGGGGACTTTT
dac 1 REVERSE	638	CCACTTCACGACCTCCTCAT
dac 2 FORWARD	699	CTTCAACCCCTCCAGTACA
dac 2 REVERSE	699	TGTCTGTCGTCGTCTTCTG
Sp6-9 FORWARD	789	CAAATGGCTCGCATGTATTG
Sp6-9 REVERSE	789	CAGTGCGTTCAAACCTCCAA

287  
288  
289  
290  
291

292

## 293 CLONING AND RNA PROBE SYNTHESIS

294 Total RNA was extracted from a large pool of *Parhyale* embryos at multiple stages of  
295 embryogenesis, from Stages 12 to 26 using Trizol. cDNA was generated using Superscript III.  
296 Primers were generated with Primer3 (<http://bioinfo.ut.ee/primer3-0.4.0>), with a preferred  
297 product size of 700bp, and did not include the DNA binding domain. Inserts were amplified with  
298 Platinum Taq (ThermoFisher 10966026), ligated into pGem T-Easy vectors (ProMega A1360),  
299 and transformed into E coli. The resulting plasmids were cleaned with a QiaPrep mini-prep kit  
300 (Qiagen A1360), and sequenced to verify the correct insert and determine sense and anti-sense  
301 promoters. In situ templates were generated by PCR from these plasmids using M13F/R primers  
302 and purified with Qiagen PCR Purification kit (Qiagen 28104). The resulting PCR products were  
303 used to make DIG-labeled RNA probes (Roche 11175025910) using either T7 or Sp6 RNA  
304 polymerase. RNA probes were precipitated with LiCl, resuspended in water, and run on an  
305 agarose gel to check that probes were the correct size, and concentration was determined using a  
306 Nanodrop 10000. Probes were used at 1-5ng/uL concentration.

307

## 308 IN SITU PROTOCOL

309 Embryo collection, fixation, and dissection as previously described<sup>53</sup>. In situ performed as  
310 previously described<sup>54</sup>. In brief, embryos were fixed in 4% paraformaldehyde (PFA) in artificial  
311 seawater for 45 minutes, dehydrated to methanol, and stored overnight at -20C to discourage  
312 embryos from floating in later hybridization solution (Hyb) step. Embryos were rehydrated to  
313 1xPBS with 0.1% Tween 20 (PTw), post-fixed for 30 minutes in 9:1 PTw:PFA, and washed in  
314 PTw. Embryos were incubated in Hyb at 55C for at least 36 hours. Embryos were blocked with  
315 5% normal goat serum and 1x Roche blocking reagent (Roche 11096176001) in PTw for 30  
316 minutes. Sheep anti-DIG-AP antibody (Roche 11093274910) was added at 1:2000 and incubated  
317 for 2 hours at room temperature. Embryos were developed in BM Purple (Roche 11442074001)  
318 for a few hours to overnight. After embryos were sufficiently developed, they were dehydrated to  
319 methanol to remove any pink background, then rehydrated to PTw. Embryos were then moved to  
320 1:1 PBS:glycerol with 0.1mg/mL DAPI, then 70% glycerol in PBS.

321

## 322 CRISPR-CAS9 GUIDE RNA GENERATION, INJECTION, AND IMAGING

323 Guide RNAs were generated using ZiFit<sup>55,56</sup> as previously described<sup>57</sup>. sgRNAs were ordered  
324 from Synthego. Injection mixes had a final concentration of 333ng/uL Cas9 protein, 150ng/uL  
325 sgRNA (for both single and double guide injection mixes), and 0.05% phenol red for  
326 visualization during injection, all suspended in water. One- or two-cell embryos were injected  
327 with approximately 40 – 60 picoliters of sgRNA mixture as previously described<sup>57</sup>. Resulting  
328 knockout hatchlings were fixed in 4% paraformaldehyde in artificial seawater at 4C for 1 – 2  
329 days, then moved to 70% glycerol in 1xPBS. Dissected hatchling limbs were visualized with  
330 Zeiss 700 and 780 confocal microscopes using the autofluorescence in the DAPI channel. Z-  
331 stacks were assembled with Volocity. Hatchling images were desaturated, levels adjusted, and  
332 false-colored using Overlay with Adobe Photoshop CS6.

333

## 334 T7 ENDONUCLEASE I ASSAY

335 Genomic primers were designed using Primer3, and flanked the target site by at least 400bp to  
336 either side. DNA isolation and subsequent PCR amplification of the region of interest was  
337 modified from previously described protocols<sup>58</sup>. Genomic DNA was amplified directly from

338 fixed hatchlings in 70% glycerol using ExTaq (Takara RR001A). The resulting PCR products  
339 were purified with the Qiaquick PCR purification kit (Qiagen 28104). Heteroduplexes were  
340 annealed and digested by T7 endonuclease I according to NEB protocols (NEB M0302L). The  
341 digested products were run out on a 1.5% agarose gel. Genomic primers used for the T7  
342 endonuclease I assay are listed below.

343

#### 344 GENOMIC DNA PRIMERS

345

Primer name	product size	seq	346
exd left	907	CTTGAGATTCGTTTCAGGTGCA	347
exd right	907	TTCTCCCCAGTTCCTTGCAA	348
hth left	943	TGTTTCGTGTACCCGCAGAT	349
hth right	943	TCGGGCATACTAGAAGGCAG	350
Sp6-9 left	935	GCCCAGCTACTAACGATTTTCA	351
Sp6-9 right	935	GATCCGCTTCCTGACAGTTG	352
Dll-e left	922	GGAATGGTGAAGGAAGAGCG	353
Dll-e right	922	TCAGCAGTGCAGACTCATGT	354
dac2 left	983	CACGCGACACTCATAACAG	355
dac2 right	983	GATGCTCCTCCCACCGAATA	356
			357
			358
			359

360

361

#### 362 PRECOXA PHYLOGENY REFERENCES

363 Branchiura<sup>59-61</sup>. Mystacocarida<sup>62,63</sup>. Ostracoda<sup>62,64-66</sup>. Copepoda<sup>62,67,68</sup>. Cirripedia<sup>66</sup>.  
364 Decapoda<sup>62,69,70</sup>. Leptostraca<sup>66</sup>. Stomatopod<sup>59,71</sup>. Amphipoda<sup>72,73</sup>. Cephalocarida<sup>59,74</sup>.  
365 Notostraca<sup>66</sup>. Spinicaudata<sup>75</sup>. Remipedia<sup>35,62</sup>. Collembola<sup>35</sup>. Insecta<sup>2,3,12,36,37,76</sup>.

366

367

368

#### 369 AUTHOR CONTRIBUTIONS

370 H.S.B. and N.H.P. conceived of the experiments. H.S.B. performed all experiments, conceived  
371 of model, and wrote the manuscript. N.H.P. edited and revised the manuscript.

372

373

374

375

376

#### 377 References

378

379

380

381

382

383

1. Matsuda, R. Morphology and Evolution of the Insect Thorax. <https://doi.org/10.4039/entm10276fv> **102**, 1–427 (1970).
2. Snodgrass, R. E. *Morphology and mechanism of the insect thorax*. **80(1)**, (1927).
3. DEUVE, T. The epipleural field in hexapods. *Annales de la Société entomologique de France* (2001).
4. Kukalová-Peck, J. Origin of the insect wing and wing articulation from the arthropodan

- 384 leg. *Can. J. Zool.* **61**, 1618–1669 (1983).
- 385 5. Snodgrass, R. E. *Principles of insect morphology*. (McGRAW-HILL BOOK  
386 COMPANY, INC., 1935).
- 387 6. Clark-Hachtel, C. M. & Tomoyasu, Y. Exploring the origin of insect wings from an evo-  
388 devo perspective. *Curr Opin Insect Sci* **13**, 77–85 (2016).
- 389 7. Requena, D. *et al.* Origins and Specification of the *Drosophila* Wing. *Current Biology*  
390 1–16 (2017). doi:10.1016/j.cub.2017.11.023
- 391 8. Prokop, J. *et al.* Paleozoic Nymphal Wing Pads Support Dual Model of Insect Wing  
392 Origins. *Curr. Biol.* **27**, 263–269 (2017).
- 393 9. Mashimo, Y. & Machida, R. Embryological evidence substantiates the subcoxal theory  
394 on the origin of pleuron in insects. *Sci Rep* **7**, 1–9 (2017).
- 395 10. Niwa, N. *et al.* Evolutionary origin of the insect wing via integration of two  
396 developmental modules. *Evol. Dev.* **12**, 168–176 (2010).
- 397 11. Averof, M. & Cohen, S. M. Evolutionary origin of insect wings from ancestral gills.  
398 *Nature* **385**, 627–630 (1997).
- 399 12. Boxshall, G. A. The evolution of arthropod limbs. *Biol. Rev.* **79**, 253–300 (2004).
- 400 13. Estella, C. A dynamic network of morphogens and transcription factors patterns the fly  
401 leg. *Curr. Top. Dev. Biol.* **98**, 173–198 (2012).
- 402 14. Estella, C., Rieckhof, G., Calleja, M. & Morata, G. The role of buttonhead and Sp1 in  
403 the development of the ventral imaginal discs of *Drosophila*. *Development* **130**, 5929–  
404 5941 (2003).
- 405 15. Campbell, G. & Tomlinson, A. The roles of the homeobox genes *aristaless* and *Distal-*  
406 *less* in patterning the legs and wings of *Drosophila*. *Development* **125**, 4483–4493  
407 (1998).
- 408 16. Angelini, D. R. & Kaufman, T. C. Functional analyses in the hemipteran *Oncopeltus*  
409 *fasciatus* reveal conserved and derived aspects of appendage patterning in insects.  
410 *Developmental Biology* **271**, 306–321 (2004).
- 411 17. Beermann, A. *et al.* The Short antennae gene of *Tribolium* is required for limb  
412 development and encodes the orthologue of the *Drosophila* *Distal-less* protein.  
413 *Development* **128**, 287–297 (2001).
- 414 18. Serano, J. M. *et al.* Comprehensive analysis of Hox gene expression in the amphipod  
415 crustacean *Parhyale hawaiiensis*. *Developmental Biology* **409**, 297–309 (2015).
- 416 19. Browne, W. E., Price, A. L., Gerberding, M. & Patel, N. H. Stages of embryonic  
417 development in the amphipod crustacean, *Parhyale hawaiiensis*. *genesis* **42**, 124–149  
418 (2005).
- 419 20. Liubicich, D. M. *et al.* Knockdown of *Parhyale* *Ultrabithorax* recapitulates evolutionary  
420 changes in crustacean appendage morphology. *Proc. Natl. Acad. Sci. U.S.A.* **106**, 13892–  
421 13896 (2009).
- 422 21. Beermann, A., Aranda, M. & Schröder, R. The Sp8 zinc-finger transcription factor is  
423 involved in allometric growth of the limbs in the beetle *Tribolium castaneum*.  
424 *Development* **131**, 733–742 (2004).
- 425 22. Schaeper, N. D., Prpic, N.-M. & Wimmer, E. A. A clustered set of three Sp-family genes  
426 is ancestral in the Metazoa: evidence from sequence analysis, protein domain structure,  
427 developmental expression patterns and chromosomal location. *BMC Evol. Biol.* **10**, 88  
428 (2010).
- 429 23. Estella, C. & Mann, R. S. Non-Redundant Selector and Growth-Promoting Functions of

- 430 Two Sister Genes, buttonhead and Sp1, in Drosophila Leg Development. *PLoS Genet* **6**,  
431 e1001001 (2010).
- 432 24. Mardon, G., Solomon, N. M. & Rubin, G. M. dachshund encodes a nuclear protein  
433 required for normal eye and leg development in Drosophila. *Development* **120**, 3473–  
434 3486 (1994).
- 435 25. Tavsanlı, B. C. *et al.* Structure–function analysis of the Drosophila retinal determination  
436 protein Dachshund. *Developmental Biology* **272**, 231–247 (2004).
- 437 26. Mito, T. *et al.* Divergent and conserved roles of extradenticle in body segmentation and  
438 appendage formation, respectively, in the cricket *Gryllus bimaculatus*. *Developmental*  
439 *Biology* **313**, 67–79 (2008).
- 440 27. Ronco, M. *et al.* Antenna and all gnathal appendages are similarly transformed by  
441 homothorax knock-down in the cricket *Gryllus bimaculatus*. *Developmental Biology*  
442 **313**, 80–92 (2008).
- 443 28. Rauskolb, C., Smith, K. M., Peifer, M. & Wieschaus, E. extradenticle determines  
444 segmental identities throughout Drosophila development. *Development* **121**, 3663–3673  
445 (1995).
- 446 29. Wu, J. & Cohen, S. M. Proximodistal axis formation in the Drosophila leg: subdivision  
447 into proximal and distal domains by Homothorax and Distal-less. *Development* **126**,  
448 109–117 (1999).
- 449 30. Prpic, N.-M. & Telford, M. J. Expression of homothorax and extradenticle mRNA in the  
450 legs of the crustacean *Parhyale hawaiiensis*: evidence for a reversal of gene expression  
451 regulation in the pancrustacean lineage. *Dev Genes Evol* **218**, 333–339 (2008).
- 452 31. Rieckhof, G. E., Casares, F., Ryoo, H. D., Abu-Shaar, M. & Mann, R. S. Nuclear  
453 translocation of extradenticle requires homothorax, which encodes an extradenticle-  
454 related homeodomain protein. *Cell* **91**, 171–183 (1997).
- 455 32. Casares, F. & Mann, R. S. The ground state of the ventral appendage in Drosophila.  
456 *Science* **293**, 1477–1480 (2001).
- 457 33. Boxshall, G. in 241–267 (Springer Berlin Heidelberg, 2013). doi:10.1007/978-3-642-  
458 36160-9\_11
- 459 34. Shultz, J. W. Morphology of locomotor appendages in Arachnida: evolutionary trends  
460 and phylogenetic implications. *Zool J Linn Soc* **97:1-56**, (1989).
- 461 35. Bäcker, H., Fanenbruck, M. & Wägele, J. W. A forgotten homology supporting the  
462 monophyly of Tracheata: The subcoxa of insects and myriapods re-visited. *Zoologischer*  
463 *Anzeiger - A Journal of Comparative Zoology* **247**, 185–207 (2008).
- 464 36. KOBAYASHI, Y. Formation of Subcoxae-1 and 2 in Insect Embryos: The Subcoxal  
465 Theory Revisited. *Proc Arthropod Embryol Soc Jpn* (2017).
- 466 37. Kobayashi, Y., Niikura, K., Oosawa, Y. & Takami, Y. Embryonic development of  
467 *Carabus insulicola* (Insecta, Coleoptera, Carabidae) with special reference to external  
468 morphology and tangible evidence for the subcoxal theory. *J. Morphol.* **274**, 1323–1352  
469 (2013).
- 470 38. Hansen, H. J. *Studies on Arthropoda*. (1930).
- 471 39. Clark-Hachtel, C. M., Linz, D. M. & Tomoyasu, Y. Insights into insect wing origin  
472 provided by functional analysis of vestigial in the red flour beetle, *Tribolium castaneum*.  
473 *Proc. Natl. Acad. Sci. U.S.A.* **110**, 16951–16956 (2013).
- 474 40. Ohde, T., Yaginuma, T. & Niimi, T. Insect morphological diversification through the  
475 modification of wing serial homologs. *Science* **340**, 495–498 (2013).

- 476 41. Medved, V. *et al.* Origin and diversification of wings: Insights from a neopteran insect.  
477 *Proceedings of the ...* (2015).
- 478 42. Wang, D. *et al.* spalt is functionally conserved in *Locusta* and *Drosophila* to promote  
479 wing growth. *Sci Rep* **7**, 1–9 (2017).
- 480 43. Shiga, Y. *et al.* Repeated co-option of a conserved gene regulatory module underpins the  
481 evolution of the crustacean carapace, insect wings and other flat outgrowths.  
482 doi:10.1101/160010
- 483 44. Bitsch, J. The controversial origin of the abdominal appendage-like processes in  
484 immature insects: Are they true segmental appendages or secondary outgrowths?  
485 (Arthropoda hexapoda). *J. Morphol.* **273**, 919–931 (2012).
- 486 45. Komatsu, S. & Kobayashi, Y. Embryonic development of a whirligig beetle, *Dineutus*  
487 *mellyi*, with special reference to external morphology (insecta: Coleoptera, Gyrinidae).  
488 *J. Morphol.* **273**, 541–560 (2012).
- 489 46. Suzuki, Y., Squires, D. C. & Riddiford, L. M. Developmental Biology. *Developmental*  
490 *Biology* **326**, 60–67 (2009).
- 491 47. Bowsler, J. H. & Nijhout, H. F. Partial co-option of the appendage patterning pathway  
492 in the development of abdominal appendages in the sepsid fly *Themira biloba*. *Dev*  
493 *Genes Evol* **219**, 577–587 (2010).
- 494 48. Hoch, H. *et al.* Non-sexual abdominal appendages in adult insects challenge a 300  
495 million year old bauplan. *Curr. Biol.* **24**, R16–7 (2014).
- 496 49. Angelini, D. R. & Kaufman, T. C. Comparative developmental genetics and the  
497 evolution of arthropod body plans. *Annu. Rev. Genet.* **39**, 95–119 (2005).
- 498 50. Moczek, A. P. On the origins of novelty in development and evolution. *Bioessays* **30**,  
499 432–447 (2008).
- 500 51. Matsuda, R. *Morphology and Evolution of the Insect Abdomen*. (Elsevier, 1976).
- 501 52. Kao, D. *et al.* The genome of *Parhyale hawaiiensis*: a model for animal development,  
502 regeneration, immunity and ligno-cellulose digestion. *Elife* 1–76 (2016).
- 503 53. Rehm, E. J., Hannibal, R. L., Chaw, R. C., Vargas-Vila, M. A. & Patel, N. H. Fixation  
504 and Dissection of *Parhyale hawaiiensis* Embryos. *Cold Spring Harbor Protocols* **2009**,  
505 pdb.prot5127–pdb.prot5127 (2009).
- 506 54. Rehm, E. J., Hannibal, R. L., Chaw, R. C., Vargas-Vila, M. A. & Patel, N. H. In Situ  
507 Hybridization of Labeled RNA Probes to Fixed *Parhyale hawaiiensis* Embryos. *Cold*  
508 *Spring Harbor Protocols* **2009**, pdb.prot5130–pdb.prot5130 (2009).
- 509 55. Sander, J. D. *et al.* ZiFiT (Zinc Finger Targeter): an updated zinc finger engineering  
510 tool. *Nucleic Acids Res.* **38**, W462–W468 (2010).
- 511 56. Sander, J. D., Zaback, P., Joung, J. K., Voytas, D. F. & Dobbs, D. Zinc Finger Targeter  
512 (ZiFiT): an engineered zinc finger/target site design tool. *Nucleic Acids Res.* **35**, W599–  
513 W605 (2007).
- 514 57. Martin, A. *et al.* CRISPR/Cas9 Mutagenesis Reveals Versatile Roles of Hox Genes in  
515 Crustacean Limb Specification and Evolution. *Curr. Biol.* **26**, 14–26 (2016).
- 516 58. Gloor, G. B., Nassif, N. A., Johnson-Schlitz, D. M., Preston, C. R. & Engels, W. R.  
517 Targeted gene replacement in *Drosophila* via P element-induced gap repair. *Science* **253**,  
518 1110–1117 (1991).
- 519 59. Schram, F. R. *Crustacea*. (Oxford University Press, USA, 1986).
- 520 60. AGUIAR, J. C. *et al.* A new species of *Argulus* (Crustacea, Branchiura, Argulidae) from  
521 the skin of catfish, with new records of branchiurans from wild fish in the Brazilian

- 522 Pantanal wetland. 1–23 (1999). doi:10.11646/zootaxa.4320.3.3  
523 61. TANZOLA, R. D., of, M. V.-O. P.-A. J.2017. *Argulus ventanensis* sp. n.(Crustacea,  
524 Branchiura) parasite of *Hypsiboas pulchellus* tadpoles (Anura, Hylidae). *panamjas.org*  
525  
526 62. Boxshall, G. Comparative limb morphology in major crustacean groups: the coxa-basis  
527 joint in postmandibular limbs. *Arthropod Relationships* (1998).  
528 63. Stachowitsch, M. & Proidl, S. *The Invertebrates*. (University of Texas Press, 1992).  
529 64. Horne, D. J. Homology and homoeomorphy in ostracod limbs. *Hydrobiologia* **538**, 55–  
530 80 (2005).  
531 65. Cohen, A. C., Martin, J. W. & Kornicker, L. S. Homology of Holocene ostracode  
532 biramous appendages with those of other crustaceans: the protopod, epipod, exopod and  
533 endopod. *Lethaia* **31:251-265**, (1998).  
534 66. Hansen, H. J. *Studies on Arthropoda. II. At the Expense of the Rask-Ørsted Fund.*  
535 (1925).  
536 67. Karanovic, T. Two new genera and three new species of subterranean cyclopoids  
537 (Crustacea, Copepoda) from New Zealand, with redescription of *Goniocyclops silvestris*  
538 Harding, 1958. *Contributions to Zoology* **74, 3/4**, 223–254 (2005).  
539 68. FIERS, F. & JOCQUE, M. Leaf litter copepods from a cloud forest mountain top in  
540 Honduras (Copepoda: Cyclopidae, Canthocamptidae). *Zootaxa* **3630**, 270–22 (2013).  
541 69. Borradaile, L. A. XXVII.— Notes upon Crustacean limbs. *Journal of Natural History*  
542 *Series 11* **17**, 193–213 (1926).  
543 70. Snodgrass, R. E. *Textbook of arthropod anatomy*. (1952).  
544 71. Watling, Les, Hof, C. H. J. & Schram, F. R. THE PLACE OF THE HOPLOCARIDA IN  
545 THE MALACOSTRACAN PANTHEON. *Journal of Crustacean Biology* **20**, 1–11  
546 (2000).  
547 72. Ungerer, P. & Wolff, C. External morphology of limb development in the amphipod  
548 *Orchestia cavimana* (Crustacea, Malacostraca, Peracarida). *Zoomorphology* **124**, 89–99  
549 (2005).  
550 73. Wolff, C. & Scholtz, G. Cell lineage analysis of the mandibular segment of the  
551 amphipod *Orchestia cavimana* reveals that the crustacean paragnaths are sternal  
552 outgrowths and not limbs. *Front. Zool.* **3**, 19 (2006).  
553 74. Olesen, J., Haug, J. T., Maas, A. & Waloszek, D. External morphology of *Lightiella*  
554 *monniotae* (Crustacea, Cephalocarida) in the light of Cambrian ‘Orsten’ crustaceans.  
555 *Arthropod Structure and Development* **40**, 449–478 (2011).  
556 75. Ferrari, F. D. & GRYGIER, M. J. Comparative morphology among trunk limbs of  
557 *Caenestheriella gifuensis* and *Leptestheria kawachiensis* (Crustacea: Branchiopoda:  
558 Spinicaudata). *Zool J Linn Soc* **139**, 547–564 (2003).  
559 76. Coulcher, J. F., Edgecombe, G. D. & Telford, M. J. Molecular developmental evidence  
560 for a subcoxal origin of pleurites in insects and identity of the subcoxain the gnathal  
561 appendages. *Sci Rep* **5**, 1–8 (2015).  
562